

NONLINEAR CHARACTERISTICS SYSTEMATIC STUDY IN PNEUMATIC ACTUATORS

Carla Silvano Ritter, carlamtmritter@yahoo.com.br

Antonio Carlos Valdiero, valdiero@unijui.edu.br

Pedro Luís Andrighetto, pedro@unijui.edu.br

Fernando Zago, fzago_egm@yahoo.com.br

UNIJUÍ, Campus Panambi, Caixa Postal 121, CEP 98280-000, Panambi - RS

Luciano Endler, lucianoka@ibest.com.br

UNIJUÍ, Rua São Francisco, 501, Caixa. Postal 560, CEP 98700-000, Ijuí - RS,

Abstract. *This paper points the main nonlinear characteristics in pneumatic actuators and presents how to address its in mathematical modeling. The pneumatic actuator is very common in industrial application because it has the following advantages: its maintenance is easy and simple, relatively low cost, self cooling properties, good power density (power/dimension rate), fast acting with high accelerations and installation flexibility. Also, compressed air is available in almost all industry plants. However, they have difficulties of control due to various nonlinear characteristics of the system, as servovalve dead zone, air flow-pressure relationship through valve orifice, air compressibility and friction effects between contact surfaces in actuator seals. The main paper contribution is to systematize its nonlinear characteristics. This systematize is important to help researches in the modeling and precision control success.*

Keywords: *pneumatic actuators; mathematical modeling; nonlinear characteristics.*

1. INTRODUCTION

This work presents the main nonlinear characteristics in pneumatic actuators and its mathematical modeling. The pneumatic actuator is very common in industrial application (Rao and Bone, 2008) because it has the following advantages: its maintenance is easy and simple, relatively low cost, self cooling properties, good power density (power/dimension rate), fast acting with high accelerations (Ningbo *et al.*, 2008) and installation flexibility. Also, compressed air is available in almost all industry plants (Uzuka *et al.*, 2009).

However, there are difficulties of control due to various nonlinear characteristics of the system (Guenther *et al.*, 2006). The nonlinearities present in pneumatic actuators are motivated by its very low stiffness (caused by air compressibility), inherently nonlinear behavior, parameter variations and low damping of the actuator systems, which make it difficult to achieve precise motion control. The main non-linearities in pneumatic servo systems are the servovalve dead zone (Valdiero *et al.*, 2008), air flow-pressure relationship through valve orifice (Rao and Bone, 2008; Endler, 2009), the air compressibility and friction effects between contact surfaces in actuator seals (Andrighetto *et al.*, 2006).

Several recent authors present a study on the characteristics of nonlinear pneumatic actuators (Perondi, 2002; Andrighetto *et al.*, 2006; Bavaresco, 2007; Rao and Bone, 2008; Endler, 2009). Valdiero *et al.* (2008) presents a mathematical model to dead zone in pneumatic servovalves, followed by the method used to compensation that is made with the addition of an inverse dead zone function in control system. Rao and Bone (2008) presents a modeling approach where they use the bipolynomial functions to model the valve flow rates, but is used a poor classical friction model. Perondi (2002) developed a nonlinear accurate model of a pneumatic servo drive with friction, where the nonlinear airflow relationship between the pneumatic valve's driving voltage and the upstream/downstream pressures. The main paper contribution is to systematize its nonlinear characteristics with some innovations such as a new equation for valve flow rate.

The paper is organized as follows. Section 2 brings a description of servo pneumatic positioning system with its main components and a schematic drawing with the nonlinearities presents in the actuator. In section 3 is shown the systematic study of the pneumatic actuator nonlinearities with the mathematical modeling. Conclusions are outlined in section 4.

2. PNEUMATIC ACTUATOR DESCRIPTION

The servo pneumatic positioning system considered in this paper is formed by a proportional servovalve and a double action rodless cylinder. This actuator permits to position one load in desired position of the actuator course or follow a desired trajectory. The Fig. 1 shows the schematic drawing of a pneumatic servo system.

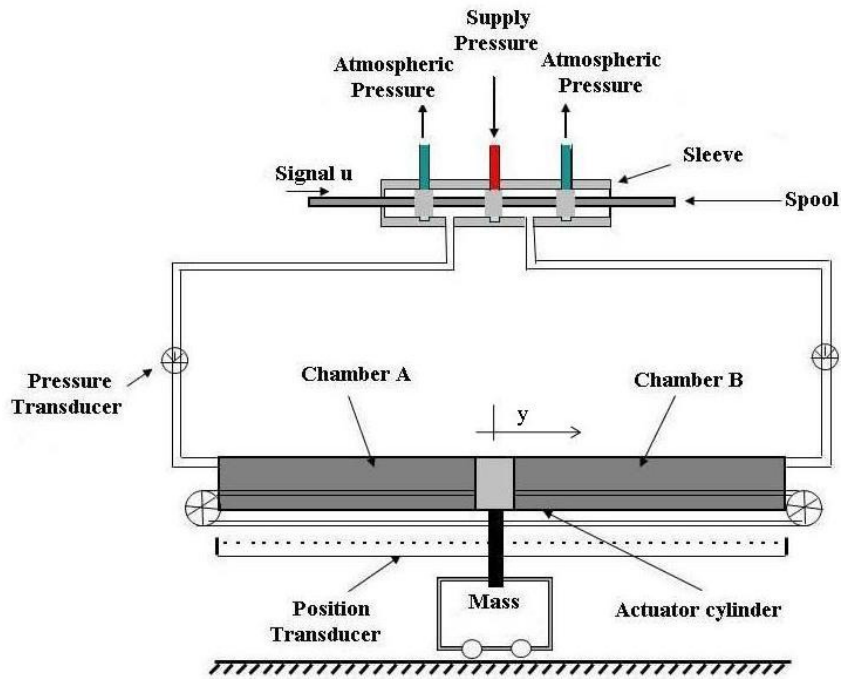


Figure 1. Schematic drawing of a pneumatic servo system

During the operation, the control signal u energizes valve's solenoid so that a resulting magnetic force is applied in the valve's spool, producing the spool displacement. The spool displacement opens control orifices so that one port is connected to the supply's pressure line and the other is connected to the atmosphere. Consequently, there is the pressure difference between cylinder chambers, resulting in a force that moves the mass M in a positive or negative displacement y , depending on the input sign.

The Fig. 2 shows block diagram of the main nonlinear parts in the dynamic model of the pneumatic actuator.

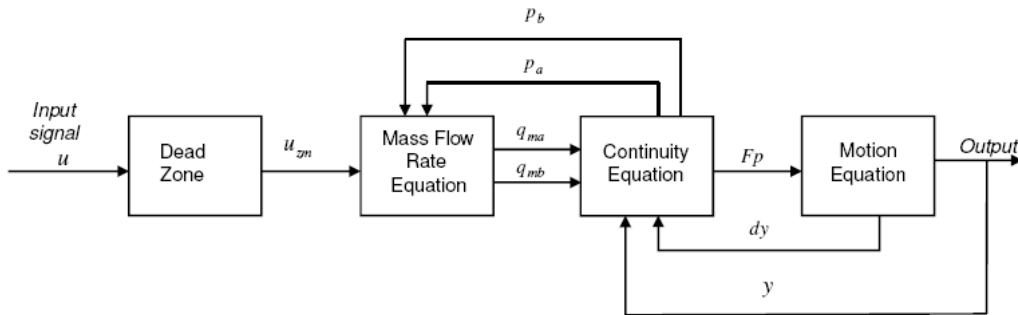


Figure 2. Block diagram of the main nonlinear parts in the dynamic model

Dead zone is common in pneumatic valves because the spool blocks valve orifices with some overlap, so that for a range of spool positions there is no air flow. It is located at the dynamic system as a block diagram shown in Fig. 2, and is characterized in section 3.1.

The air flow-pressure relationship through valve orifice is a nonlinear function that depends on pressure difference across the valve orifice and valve opening. In this paper, we present a new mass flow rate equation in section 3.2.

The pressures dynamic model is obtained from continuity equation and results in nonlinear first order differential equation. This dynamic behavior depends on pneumatic cylinder size. Small cylinder bore size produces significant effects (Rao and Bone, 2008) such as it results in a faster pressure response, the bore size is reduced the ratio of friction force to maximum pneumatic force increases, and the chamber pressures are more sensitive to small variations in the mass flow rate. Therefore the precise tracking control is more difficult with smaller bore sizes. This detail nonlinear dynamics is presented in section 3.3.

The nonlinear friction is the more important factor that affects the motion equation. Friction is a nonlinear phenomenon difficult to describe analytically. The friction often changes with time and may depend in an unknown way on environmental factors, such as temperature and lubricant condition. Even so is important the modeling of their main

characteristics. In this paper, we consider the actuator friction dynamics described by the LuGre model, proposed in Canudas *et al.* (1995) and improved by Dupont *et al.* (2000) in order to include stiction effects. This model is presented in section 3.4.

3.MATEMATICAL MODELING OF PNEUMATIC ACTUATOR NONLINEARITIES

This section presents the systematic study of the pneumatic actuator nonlinearities with the mathematical modeling. The system constitutes a fifth order nonlinear dynamic model of the pneumatic positioning system and considers the nonlinearity of the dead zone, the mass flow rate, the pressure dynamic and the motion equation, that includes the friction dynamics.

3.1. Dead Zone

This section presents the mathematical model for dead zone nonlinearity and its graphical representation. Dead zone is a static input-output relationship which for a range of input values gives no output. The Fig. 3 shows a sectional view sketch of typical spool valve with main mechanical elements.

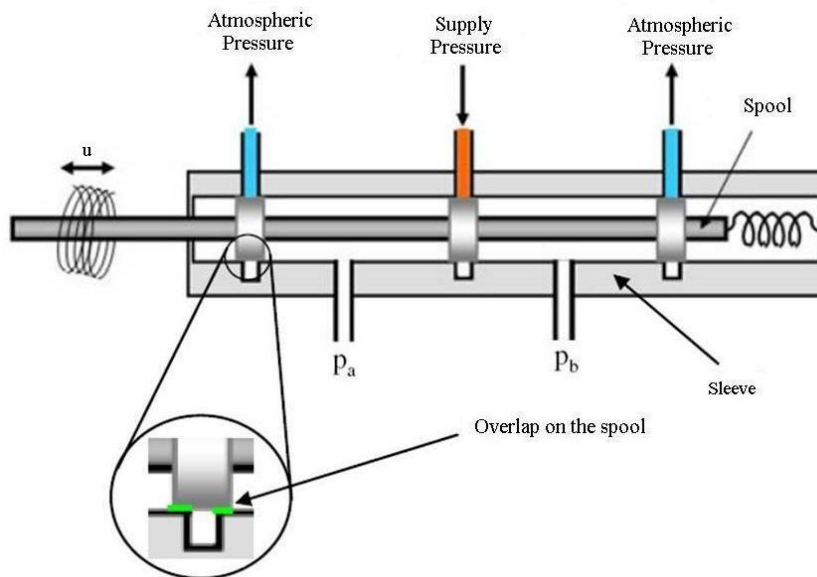


Figure 3. Sectional view sketch of typical spool valve with main mechanical elements of the proportional valve with input dead zone

The mathematical model for dead zone in pneumatic servovalves presented in this section was obtained from Tao and Kokotovic (1996).

The dead zone analytical expression is given by the equation:

$$u_{zm}(t) = \begin{cases} md(u(t) - z_{md}) & \text{se } u(t) \geq z_{md} \\ 0 & \text{se } z_{me} < u(t) < z_{md} \\ me(u(t) - z_{me}) & \text{se } u(t) \leq z_{me} \end{cases} \quad (1)$$

where u is the input value, u_{zm} is the output value, z_{md} is the right limit of dead zone, z_{me} is the left limit of dead zone, md is the right slope of output and me is the left slope of output.

Figure 4 shows a graphical representation of dead zone. In general, neither the break-points (z_{md} and z_{me}) nor the slopes (md and me) are equal.

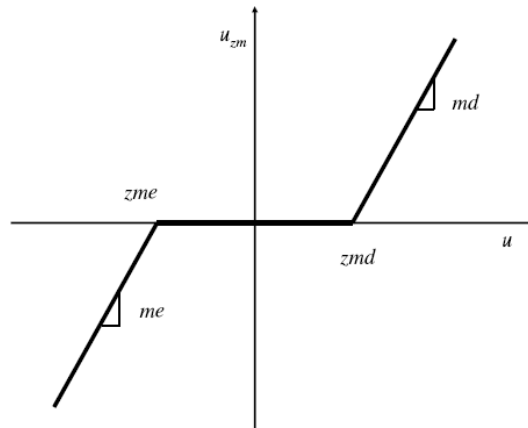


Figure 4. Graphical representation of the dead zone

In current fluid power literature, dead zone in valves is expressed as a percentual of spool displacement. Bavaresco (2007) has identified dead zone values for this valve after transforming the valve control input range to -10 V to + 10 V with the addition of a compensation block in the controller. They are $zmd = zme = 0,88$ V, with zero position = 0,1 V. The md and me parameters have been adjusted to unit values.

3.2. Mass Flow Rate

According to Rao and Bone (2008), the mass flow rate model of the proportional valve is a key part of the system model. In this paper, we use an innovator model to mass flow rate equation q_{ma} and q_{mb} developments by Endler (2009), given by equations:

$$q_{ma}(u, p_a) = g_1(p_a, \text{sign}(u)) \arctg(2u) \quad (2)$$

$$q_{mb}(u, p_b) = g_2(p_b, \text{sign}(u)) \arctg(2u) \quad (3)$$

where g_1 and g_2 are signal functions given by

$$g_1(p_a, \text{sign}(u)) = \beta \Delta p_a = \begin{cases} (p_{\text{sup}} - p_a) \beta^{\text{ench}} & \text{se } u \geq 0 \\ (p_a - p_{\text{atm}}) \beta^{\text{esv}} & \text{se } u < 0 \end{cases} \quad (4)$$

$$g_2(p_b, \text{sign}(u)) = \beta \Delta p_b = \begin{cases} (p_{\text{sup}} - p_b) \beta^{\text{ench}} & \text{se } u < 0 \\ (p_b - p_{\text{atm}}) \beta^{\text{esv}} & \text{se } u \geq 0 \end{cases} \quad (5)$$

where p_{sup} is the supply pressure, p_{atm} is the atmospheric pressure and β^{ench} and β^{esv} are the constant coefficients.

The Eq. (2) and (3) are a fitting of a surface obtained experimentally (Endler, 2009), considering that the piston is stopped, in that way the volume is constant and the speed of the piston is null. The mass flow rates at different pressures and valve input voltages were first estimated from the pressure versus time responses obtained for step inputs in valve voltage and a fixed piston position.

The fitted mass flow rate in valve orifice, q_{ma} , is plotted versus input voltage and pressure difference in Fig. 5.

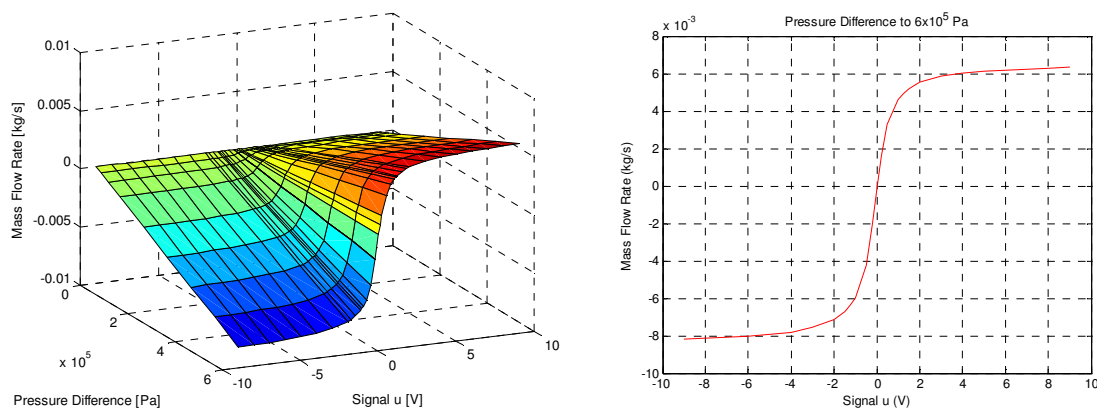


Figure 5. Fitted model of mass flow rate

Rao and Bone (2008) used a 2nd order bipolynomial equation to fit this function. In a similar way, Perondi (2002) used a third order polynomial one. Bobrow and McDonell (1998) use a curve fit for the change in internal energy as a function of cylinder pressure which is quadratic in u . One of the greatest problems in these equations found in the literature is the difficulty in isolate the signal u , necessary when is used a control methodology that considers the nonlinear characteristics of the system.

The equations to mass flow rate proposed by Endler (2009) are innovations that possess advantages as easiness of computational implementation and differentiation.

3.3. Pressure Dynamics

The cylinder used in this modeling is symmetric and without spindle. In mathematical modeling the pressure changes in the chambers are obtained using energy conservation laws. The Fig. 5 shown a schematic drawing of cylinder used.

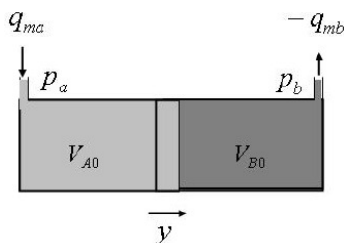


Figure 5. Cylinder's schematic drawing

The relationship between the air mass flow rate and the pressure changes in the chambers is obtained using energy conservation laws. According to Perondi (2002), the energy balance yields

$$q_{ma} T - \frac{p_a}{C_p} \frac{dV_a}{dt} = \frac{1}{\gamma R} \frac{d}{dt} (p_a V_a) \quad (6)$$

where T is the air supply temperature, q_{ma} is the air mass flow rate into chamber A, p_a is the absolute pressure in chamber A, C_p is the specific heat of the air at constant pressure, C_v is the specific heat of the air at constant volume $\gamma = C_p/C_v$ is the ratio between the specific heat values of the air, R is the universal gas constant, $\dot{V}_a = (dV_a/dt)$ is the volumetric flow rate. Assuming that the mass flow rates are nonlinear functions of the servovalve control voltage (u) and of the cylinder pressures, that is, $q_{ma} = q_{ma}(p_a, u)$ and $q_{mb} = q_{mb}(p_b, u)$.

The total volume of chamber A is given by

$$V_a = A y + V_{a0} \quad (7)$$

where A is the cylinder cross-sectional area, y is the piston position and V_{a0} is the dead volume of air in the line and at the chamber A extremity, include the pipeline. The change rate for this volume is $\dot{V}_a = A\dot{y}$, where \dot{y} is the piston velocity.

In this manner, calculating the derivative term in the right hand side of Eq. (6), and using $C_p = (\gamma R)/(\gamma - 1)$ we can solve this equation to obtain

$$\dot{p}_a = -\frac{A \gamma \dot{y}}{A y + V_{a0}} p_a + \frac{R \gamma T}{A y + V_{a0}} q_{ma}(p_a, u) \quad (8)$$

Similarly for chamber B of the cylinder we obtain

$$\dot{p}_b = \frac{A \gamma \dot{y}}{V_{b0} - A y} p_b - \frac{R \gamma T}{V_{b0} - A y} q_{mb}(p_b, u) \quad (9)$$

3.4. Friction Dynamics in motion equation

Applying Newton's second law to the piston-load assembly results in

$$M \ddot{y} + F_{atr} = F_p \quad (10)$$

where M is the mass of the piston-load assembly, \ddot{y} is the cylinder acceleration, F_{atr} is the friction force, F_p is the pneumatic force related to the pressure difference between the two sides of the piston, that is given by $A(p_a - p_b)$.

In this section the dynamic model to friction is based in the microscopic deformation of asperities in surface contact. It is possible to perceive an evolution in friction models that are based in the asperity microscopic deformations and depicted in recent papers.

The Dahl model describes friction in the presliding movement phase, in similar way with the rigid spring with damping behavior, but has not included the Stribeck friction effect. The LuGre model, proposed by Canudas-De-Wit *et al* (1995), is an improved model that includes the Stribeck Friction and describes many complex friction behaviors, but is limited in the presliding movement phase, according to simulations results presented by Dupont *et al.* (2000) and experimental texts carried out by Swevers *et al.* (2000). These authors propose also improvements in LuGre model through the inclusion of a model to hysteresis with non local memory and sliding-force transition curves in presliding movement phase. This improved model is named Leuven model and used in friction modeling to a pneumatic servo positioning system by Nouri *et al.* (2000). Dupont *et al.* (2000) also propose improvements in LuGre model through its interpretation as an elasto-plastic friction model that are used in this paper.

Figure 6 represents the contact between surfaces through a lumped elastic asperity, considering a rigid body where the displacement y is decomposed into its elastic and plastic (inelastic) components z and w .

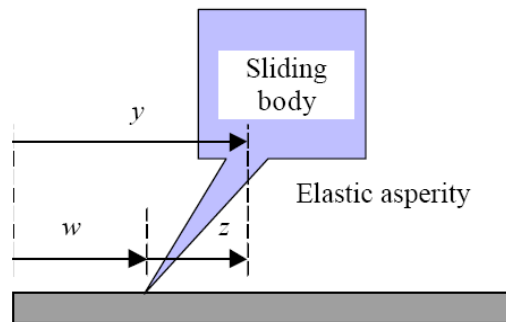


Figure 6. Model of body subject to friction force showing elastic (z) and inelastic (w) displacement components

The friction force is described according to the LuGre friction model proposed by Canudas-de-Wit *et al.* (1995). In this model the friction force is given by

$$F_{atr} = \sigma_0 \dot{z} + \sigma_1 z + \sigma_2 \dot{y} \quad (11)$$

where z is a friction internal state that describes the average elastic deflection of the contact surfaces during the stiction phases, σ_0 is the stiffness coefficient of the microscopic deformations z during the presliding displacement, σ_1 is a damping coefficient, σ_2 represents the viscous friction, \dot{y} is the velocity

The dynamics \dot{z} of the internal state z is modeled by the equation

$$\frac{dz}{dt} = \dot{y} - \alpha(z, \dot{y}) \frac{\sigma_0}{g_{ss}(\dot{y})} |\dot{y}| z \quad (12)$$

where $g_{ss}(\dot{y})$ is a positive function that describes the steady-state characteristics of the model for constant velocity motions and is given by

$$g_{ss}(\dot{y}) = F_c + (F_s - F_c) e^{-\left(\frac{\dot{y}}{\dot{y}_s}\right)^2} \quad (13)$$

where F_c is the Coulomb friction force, F_s is the static friction force and \dot{y}_s is the Stribeck velocity. Figure 7 illustrate the behavior of the friction force as a function of velocity in steady-state (Valdiero *et al.*, 2005).

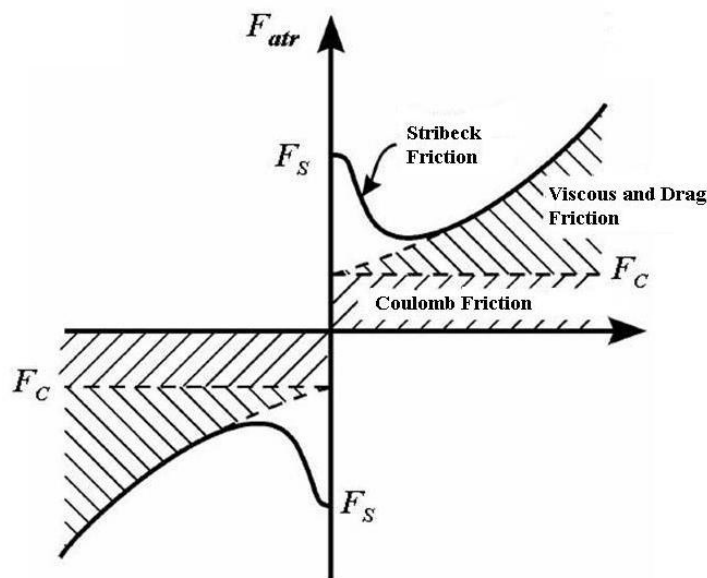


Figure 7. Friction force characteristics combined in steady-state

The function $\alpha(z, \dot{y})$ is presentation according Dupont *et al.* 2000 and is used to represent the stiction. This function is defined by equations

$$\alpha(z, \dot{y}) = \begin{cases} 0, & \text{if } |z| \leq z_{ba} \\ 0 < \frac{1}{2} \operatorname{sen} \left(\pi \frac{z - \left(\frac{z_{\max}(\dot{y}) + z_{ba}}{2} \right)}{z_{\max}(\dot{y}) - z_{ba}} \right) < 1, & \text{if } z_{ba} < |z| < z_{\max}(\dot{y}) \\ 1, & \text{if } |z| \geq z_{\max}(\dot{y}) \\ 0, & \text{if } \operatorname{sgn}(\dot{y}) \neq \operatorname{sgn}(z) \end{cases} \quad \left. \begin{array}{l} \operatorname{sgn}(\dot{y}) \\ = \\ \operatorname{sgn}(z) \end{array} \right\} \quad (14)$$

$$0 < z_{ba} < z_{\max}(\dot{y}) = \frac{g_{ss}(\dot{y})}{\sigma_0} \quad \text{para } \forall \dot{y} \in \Re \quad (15)$$

where z_{ba} is a breakaway displacement, such that to $z \leq z_{ba}$, all movements in friction interface consists in elastic displacements only and z_{max} is the maximum value of microscopic deformations and is velocity dependent.

Is possible to note that, with z represented by Eq. (14), when sliding movement is in steady state, \dot{y} is constant, $\alpha(z, \dot{y}) = 1$ and $\dot{z} = 0$. The z states values is approaches by equation:

$$z_{ss} = \frac{\dot{y}}{|\dot{y}|} \frac{g_{ss}(\dot{y})}{\sigma_0} = \text{sgn}(\dot{y}) \frac{\left(F_c + (F_s - F_c) e^{-\left(\frac{\dot{y}}{\dot{y}_s}\right)^2} \right)}{\sigma_0} \quad (16)$$

Substituting the equation (16) into equation (14) is obtained the friction force at steady state:

$$F_{atrss} = \sigma_0 z_{ss} + \sigma_1 \cdot 0 + \sigma_2 \dot{y} = \text{sgn}(\dot{y}) \left(F_c + (F_s - F_c) e^{-\left(\frac{\dot{y}}{\dot{y}_s}\right)^2} \right) + \sigma_2 \dot{y} \quad (17)$$

This dynamic properties of friction model presented are shown by Dupont *et al.* (2000) and follow similar analysis carried out by Lyapunov method, as presented by Canudas-De-Wit *et al.* 1995 and Canudas-De-Wit (1998). Among model main properties, is cited that z state variable is limited, the model is dissipative, satisfies the stick and slip conditions and represents adequately the pre-sliding movement phase.

The applied force of Fig. (8a) was chosen to challenge the stiction capability of the model, the force ramps up to cause break-away, and then returns to a level below that of Coulomb friction. Additionally, an oscillation is present such as could be introduced by sensor noise or vibration. The response of friction model is seen in Fig. (8b). The friction dynamic model renders both presliding displacement and stiction.

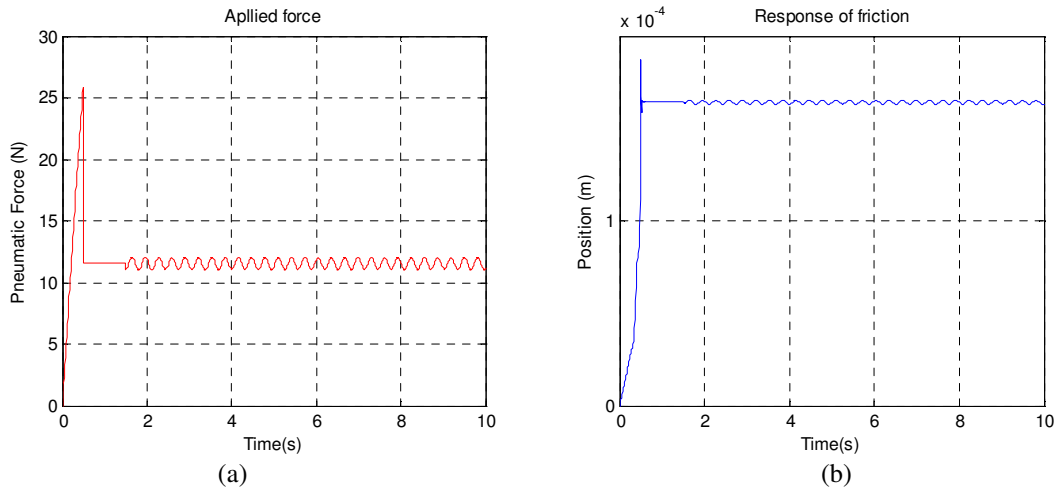


Figure 8. Applied force in pneumatic actuator and position response in both presliding displacement and stiction

4. CONCLUSIONS

In this paper was presented nonlinear characteristics systematic study in pneumatic actuators and how to address its in mathematical modeling. There was bibliographical revision in recent literature. However, these studies don't address all nonlinearities. So, the main paper contribution was present its nonlinearities and their completed mathematical modeling with some innovation. This systematize is important to help researches in the modeling and precision control success. Future research will include a control strategy to overcome nonlinearity problems of the pneumatic system.

5. ACKNOWLEDGEMENTS

This work has the financial support of Brazilian governmental agency CNPq (Conselho Nacional de Desenvolvimento Científico e Tecnológico). Authors also wish to express gratitude to FAPERGS (Fundação de Amparo à Pesquisa do Estado do Rio Grande do Sul) and UNIJUÍ.

6. REFERENCES

- Andrighetto, P. L., Valdiero, A. C., Carlotto, L., 2006, "Study of the friction behavior in industrial pneumatic actuators", In: ABCM Symposium Series in Mechatronics, ed. Rio de Janeiro: ABCM Brazilian Society of Mechanical Sciences and Engineering, Vol. 2, pp. 369-376.
- Bavaresco, D., 2007, "Mathematical modeling and control of a pneumatic actuator", (In Portuguese), Master Thesis, Mathematical Modeling Master Course, Unijuí - Regional University of Northwestern Rio Grande do Sul State, Brazil.
- Bobrow, J. E., McDonell, B. W., 1998, "Modeling, Identification, and Control of a Pneumatically Actuated, Force Controllable Robot", IEEE Trans. on Robotics and Automation, Vol. 14, No. 5, pp. 732-742.
- Canudas de Wit, C., Olsson, H., Astrom, K.J. and Lischinsky, P., 1995, "A New Model for Control Systems with Friction", IEEE Transactions on Automatic Control, Vol. 40, No. 3, pp.419-425.
- Canudas-De-Wit, C., 1998, Comments on "A new model for control of systems with friction", IEEE Transactions on Automatic Control, Vol. 43, No. 8, pp.1189-1190.
- Dupont, P., Armstrong, B., Hayward, V., 2000, "Elasto-plastic friction model: contact compliance and stiction", Proceedings of the American Control Conference, Illinois, United States of America, pp. 1072-1077.
- Endler, L., 2009, "Mathematical modeling of the mass flow rate of a pneumatic servovalve and its application in the optimal control of a pneumatic position servosystem", (In Portuguese), Master Thesis, Mathematical Modeling Master Course, UNIJUÍ – Regional University of Northwestern Rio Grande do Sul State, Brazil.
- Guenther, R., Perondi, E. A., DePieri, E. R., Valdiero, A. C., 2006, "Cascade Controlled Pneumatic Positioning System with LuGre Model Based Friction Compensation", Journal of the Brazilian Society of Mechanical Engineering, Vol. 28, No. 1, pp. 48-57.
- Ningbo Yu, Hollnagel, C., Blickenstorfer, A., Kollias, S.S., Riener, R., 2008, "Comparison of MRI-Compatible Mechatronic Systems With Hydrodynamic and Pneumatic Actuation", IEEE/ASME Transactions on Mechatronics, Vol. 13, No. 3, pp. 268 – 277.
- Nouri, B., Al-Bender, F., Swevers, J., Vanherck, P. and Van Brussel, H., 2000, "Modeling a Pneumatic Servo Positioning System with Friction", Proceedings of the ACC 2000, pp. 1067-1071.
- Perondi, E.A., 2002, "Cascade Nonlinear Control with Friction Compensation of a Pneumatic Servo Positioning" (In Portuguese), PhD Thesis, Mechanical Engineering Department, Federal University of Santa Catarina, Brazil, 178p.
- Rao, Z., Bone, G.M., 2008, "Nonlinear Modeling and Control of Servo Pneumatic Actuators Control Systems Technology", In IEEE Transactions on Control System Technology, Vol. 16, No. 3, pp.562-569.
- Swevers, J., Al-Bender, F., Ganseman, C. G., Prajogo, T., 2000, "An integrated friction model structure with improved presliding behavior for accurate friction compensation", In IEEE Transactions on Automatic Control, Vol. 45, No. 4, pp. 675-686.
- Tao, G. and Kokotovic, P.V., 1996, "Adaptive control of systems with actuator and sensor nonlinearities", New York: John Wiley & Sons, 294 p.
- Uzuka, K., Enomoto, I., Suzumori, K., 2009, "Comparative Assessment of Several Nutation Motor Types Mechatronics", IEEE/ASME Transactions on Mechatronics, Vol. 14, No. 1, pp. 82-92.
- Valdiero, A. C., Andrighetto, P. L., Carlotto, L., 2005, "Dynamic modeling and friction parameters estimation to pneumatic actuators", Proceedings of MUSME 2005, the International Symposium on Multibody Systems and Mechatronics, Uberlandia, Brazil.
- Valdiero, A. C., Bavaresco D., Andrighetto, P. L., 2008, "Experimental identification of the dead zone in proportional directional pneumatic valves", International Journal of Fluid Power, Vol.9, pp. 27-34.

7. RESPONSIBILITY NOTICE

The authors are the only responsible for the printed material included in this paper.